GLASS-GRAPHITE COMPOSITE MATERIALS

M.Z.H. MAYZAN, J.W. LLOYD, P.G. HEATH, M.C. STENNETT, N.C. HYATT and R.J. HAND

Immobilisation Science Laboratory, Department of Materials Science and Engineering, University of Sheffield, United Kingdom

Abstract

A summary is presented of investigations into the potential of producing glass-composite materials for the immobilisation of graphite or other carbonaceous materials arising from nuclear power generation. The methods are primarily based on the production of base glasses which are subsequently sintered with powdered graphite or simulant TRISO particles. Consideration is also given to the direct preparation of glass-graphite composite materials using microwave technology. Production of dense composite wasteforms with TRISO particles was more successful than with powdered graphite, as wasteforms containing larger amounts of graphite were resistant to densification and the glasses tried did not penetrate the pores under the pressureless conditions used. Based on the results obtained it is concluded that the production of dense glass-graphite composite wasteforms will require the application of pressure.

1. INTRODUCTION

Vitrification of radioactive wastes is a well established technique used for a range of often chemically complex wastes, often high level wastes, in countries including the UK, US and France [1,2]. An appropriate choice of glass composition results in a durable wasteform that can incorporate a wide range of waste elements, which are chemically bonded into the glass structure. Vitrification also offers significant volume reduction.

Some wastes are, however, difficult to incorporate into durable glass compositions and thus there has been increasing interest in the production of glass-composite materials in which the problematic waste is either directly encapsulated [3,4,5] or becomes part of an encapulsated crystal phase [6].

Irradiated graphite and other carbonaceous wastes are not, in general, readily incorporated into silicate melts and are therefore difficult to incorporate into vitreous wasteforms by conventional glass processing routes. Glass-composite wasteforms offer an alternative approach that is of interest for the production of vitreous glass-graphite wasteforms, in which the irradiated graphite is encapsulated rather than fully bonded into the resultant composite wasteform. Such wasteforms could also be attractive for high activity TRISO particles from irradiated HTR fuels.

A series of studies on the production of glass-graphite composite wasteforms are summarised in the following.

2. EXPERIMENTAL METHODS

2.1 Microwave sintering of glass-graphite composites

Initial studies were based on using graphite as the microwave susceptor. It was found however, that although powdered graphite did suscept sufficiently to give notable heating, once the graphite had been pressed into a pellet form (with or without other raw materials) such heating was too limited to

enable glass formation. As a result subsequent work concentrated on the production of glasses from raw materials that included another suscepting raw material, as well as graphite. On this basis the viability of microwave vitrification for a range of base silicates, borosilicates and phosphate glasses was examined. Following this initial assessment an iron phosphate base glass using Fe_3O_4 as a susceptor and the results obtained using this glass are described here.

Iron phosphate glass composites with a nominal base glass composition of $40Fe_2O_3 \cdot 60P_2O_5$ (mol%) containing up to 38 wt% powdered graphite were prepared using a domestic microwave oven (DMO). The DMO had a maximum 800 W power output at a frequency of 2.45 GHz. The composites were prepared from laboratory grade Fe_3O_4 (97% pure, Alfa Aesar), $NH_4H_2PO_4$ (98% pure, Alfa Aesar) and an industrial grade of powdered graphite obtained from China as the irradiated graphite waste simulant. In all cases, batches sufficient to produce 3 g samples were weighed, mixed and manually ground using an agate mortar and pestle for approximately 5 minutes to ensure homogeneity of the samples. 2 g of the batches were uniaxially pressed, without binder, in a 13 mm diameter die with a pressure of 3 tons. The pressed pellets were placed in mullite crucibles with vitreous silica lids and the lidded crucible containing the pellet was placed inside a recessed alumina block mounted on alumina spacers inside the DMO. The block was positioned in such a way as to ensure that the maximum amount of the electromagnetic wave could be absorbed by the samples. Pellets were then irradiated at maximum power for times up to 20 minutes either in air or argon. For processing under argon the DMO was placed in a glovebox. After processing the alumina block was removed from the microwave cavity and the pellets were taken out from the crucible to maximise the cooling rate. Processed samples were kept dry and characterised.

2.2 Sintering of glass-graphite composites

For conventional sintering the range of base glasses detailed in table 1 were initially prepared by using conventional glass melting. The iron phosphate (FeP) composition was selected for comparison with the microwave sintered samples. JL1 is a glass reported in [7] as being relatively compatible with graphite, the aluminoborosilicate (ABS) glass was selected because it had been found to be compatbile with simulated TRISO fuel particles [8] (and see sections 2.3 and 3.3 below). G11 is a glass reported in [9,10], which has been investigated for the immobilisation of intermediate level waste (ILW), and the calcium aluminosilicate (CAS) glass has good chloride retention [11] and is thus potentially of interest for retaining any ^{36}Cl present in the irradiated graphite. Using a natural glass such as obsidian would avoid the need for an additional melting process step as compared to using man-made base glasses.

TABLE 1: BATCHED GLASS COMPOSITIONS (MOL%) FOR THE BASE GLASSES FOR CONVENTIONAL SINTERING (NB: OBSIDIAN IS AN ANALYSED COMPOSITION OF A NATURAL PRODUCT, WHICH WAS ALSO FOUND TO INCLUDE 0.57 MOL% Cl)

Oxide	**Glass code**					
	JL1	**ABS-1**	**G11**	**CAS**	**Obsidian**	**FeP**
Li_2O	11.60		9.70			
Na_2O	19.20	7.50	15.59		4.43	
K_2O	0.83				3.47	
MgO		1.61				
CaO	3.88	2.99		51.40	0.88	
BaO	7.63					
ZnO	5.60					
Fe_2O_3			5.00		0.60	40.00
Al_2O_3	1.47	5.30	2.60	7.16	8.36	
P_2O_5						60.00
B_2O_3	19.92	7.50	9.20			
SiO_2	29.87	75.12	57.90	41.44	81.70	

Oxide	Glass code					
	JL1	ABS-1	G11	CAS	Obsidian	FeP
Melting temperature /ºC	1200	1600	1100	1450	-	1150
Melting time /h	5	3	3	5	-	3
Density /g cm^{-3}	2.913 ±0.005	2.310 ±0.003	2.573 ±0.006	2.878 ±0.009	2.360 ±0.003	3.161 ±0.001
T_g /ºC	512	588	411	792	659	474
Sintering T /ºC	550	790	560	890	960	770

For all the man-made glasses batches sufficient to produce 300 g glass were placed in a preheated mullite crucible and melted as detailed in table 1. 1 hour was allowed for the melts to become batch free after which they were stirred at ~60 rpm using a mullite stirrer. Glass frints were produced by quneching the melt into water. The glass frits were dried, crushed using a stainless steel precursor mortar and sieved <75µm. 2 g batches consisting of 80 wt% powdered glass and 20 wt% graphite were mixed thoroughly and then pressed in a similar fashion as described in section 2.1. The pellets were then sintered in argon initially at various sintering temperatures with a 2 hour dwell and 5ºC min^{-1}. heating and cooling rates. The effects of different graphite waste loadings with all glasses apart from JL1 were also studied; these tests were conducted at the sintering temperatures given in table 1 which were identified as giving the maximum densification with the 20 wt% loaded samples.

2.3 Sintering of glass-TRISO particle composites

Simulant TRISO particle-fuel particles, with a surrogate ZrO_2 core, supplied by Necsa (South African Nuclear Energy Corporation) were used. Three base soda-lime-silica (SLS) glasses and an aluminoborosilicate (ABS) glass composition were prepared (see table 2 for compositional details). The SLS glasses were prepared from industrial grade reagents (SiO_2, Na_2CO_3, $CaCO_3$, H_3BO_3 and $4MgCO_3 \cdot Mg(OH)_2 \cdot 5H_2O$). After solidification the glasses were crushed.

TABLE 2: ANALYZED GLASS COMPOSITIONS (MOL%) USED TO PREPARE SINTERED GLASS-TRISO PARTICLE COMPOSITES

Oxide	Glass code			
	SLSA	SLSB	SLSC	ABS-1
SiO_2	68.23	74.86	76.76	72.20
Na_2O	13.31	12.73	13.04	7.10
CaO	12.90	8.70	4.52	2.60
B_2O_3	1.72	1.20	1.53	8.20
Al_2O_3	1.75	0.14	0.71	8.60
MgO	ND	ND	2.32	0.10
Density /g cm^{-3}	2.578 ± 0.003	2.535 ± 0.003	2.486 ± 0.003	2.360 ± 0.003
TEC /10^{-6} K^{-1}	11.4 ± 0.2	11.2 ± 0.2	10.6 ± 0.2	7.2 ± 0.2
T_g /°C	595 ± 5	583 ± 5	555 ± 5	610 ± 5

Both glass and glass-TRISO pellets were produced by uniaxially pressing powdered glass, or powdered glass plus 10 wt% simulant TRISO particles in a 13 mm diameter die with a pressure of 3 tons. The pellets were sintered in a tube furnace either under air or under a reducing (95% N_2, 5% H_2)

atmosphere at temperatures between 650°C and 750°C for times of 15 to 60 minutes. The heating and cooling rates were 2ºC min^{-1}.

2.4 Characterisation methods

Powder X-ray diffraction was used to confirm the amorphous nature of the glasses and to identify any crystal phases that were present in the composite materals. A Siemens D500 or D5000 diffractometer and CuK_α radiation, over a range $10° < 2\theta < 60°$ or $10° < 2\theta < 80°$ with a step size of 0.02º or 0.05º respectively was used. Bulk densities of the materials were measured using Archimedes' principle with water as the immersion fluid; densities of powdered samples were determined using helium pycnometry.

Glass transition temperatures (T_g) were determined by differential thermal analysis (DTA) using a Perkin Elmer DTA7. Samples were heated from 25 to 1000°C at a heating rate of 10°C min^{-1}. The extrapolated onset method was used to determine T_g using the Netzsch Pyris software package. Compositional analysis was performed using X-ray Fluorescence Spectroscopy (XRF) on a Phillips PW2404 XRF Axios.

Sintered composites were sectioned with a diamond edged slow saw, resin mounted, successively ground and polished to a 1 µm finish for examination with optical microscopy. Grinding was performed using either 120, 400, 800 and 2400 grit SiC papers or 600 and 1000 grit diamond matrix plates and polishing using 6, 3, 1 µm diamond pastes. Cross sectioned surfaces were examined using either optical or scanning electron microscopy (SEM). Optical microscopy was performed on a Reichert-Jung Polyvar Met microscope equipped with a Zeiss AxioCam MRc. SEM was performed using a JOEL 6400 SEM equipped with an energy dispersive X-ray spectrometer (EDS).

3. RESULTS

3.1 Iron phosphate glass and glass-graphite composites

No evidence of crystalline phases was found by XRD in samples of the base iron phosphate glass composition after microwaving for 8 minutes or greater; similar X-ray patterns were obtained for the microwaved and conventionally melted iron phosphate base glasses. The powdered densities of glasses produced from the conventional and microwave melting processes were 3.16 and 3.00 g cm^{-3}, respectively.

Iron phosphate glass graphite composite pellets microwaved for 1, 2 and 3 minutes show increasing mass losses of 17.6 ± 1.8, 24.1 ± 2.4 and 26.9 ± 2.7 %, indicating the removal of volatile components from the glass batch (NH_3 and H_2O). After 4 minutes microwave processing, the mass change of the microwave heated pellets was 28.2 ± 2.8 % and there was no significant further change as the microwave processing time was increased from 4 to 20 minutes. Similar results were obtained for processing in air or argon (see table 3). The mass loss of the glass composites has been compared with the experimental mass loss for full transformation of the raw materials to glass by microwave melting. This comparison indicates that up to ~2.5 % of graphite may have oxidised when microwave heated for times between 4 and 20 minutes. However, as can be seen from table 3, the porosity of the glass-graphite composites remained high at about 38% for 20wt% graphite and even higher for higher waste loadings. Again processing in air or in argon had little or no effect on the measured porosity. In comparison samples conventionally sintered at 770ºC for 2 h exhibited much lower porosity levels of about 15%. This conventionally sintered sample also exhibited less graphite oxidation; estimated to be about 0.6%.

TABLE 3: PHYSICAL PROPERTIES OF IRON PHOSPHATE GLASS-GRAPHITE COMPOSITES

Sample	**Measured mass loss /%**	**Expected mass loss /%**	**Bulk density / g cm^{-3}**	**Powdered density / g cm^{-3}**	**Porosity /%**
DMO 38 wt% graphite, 20 min	22.9 ± 2.3	21.2	1.6 ± 0.2	2.8 ± 0.1	42.8 ± 4.3
DMO 30 wt% graphite, 20 min	25.8 ± 2.6	23.8	1.6 ± 0.2	2.9 ± 0.1	45.8 ± 4.6
DMO 20 wt% graphite, 20 min	29.0 ± 2.9	26.7	1.9 ± 0.2	3.2 ± 0.2	36.9 ± 3.7
DMO 20 wt% graphite, 20 min (Ar)	29.2 ± 2.9	26.7	1.9 ± 0.2	3.0 ± 0.2	37.5 ± 3.8
CPS 20 wt% graphite, 2h at 770°C (Ar)	0.6 ± 0.1	-	2.6 ± 0.3	3.1 ± 0.2	14.9 ± 1.5

Figure 1 shows the XRD spectra of iron phosphate glass composites that contain 20 wt% graphite produced using various exposure times, environments and sintering methods. Graphite peaks can be seen in all of the XRD spectra. For all of the microwaved samples, mixtures of $Fe_2P_2O_7$, $Fe(PO_3)_3$ and FeP_2O_6 crystals were identified, in addition traces of Fe_2O_3, $NH_4H_2PO_4$ and Fe_3O_4 were also identified in samples microwaved for 1 to 3 minutes. It can be seen that the peaks related to iron phosphate crystalline phases become sharper and more pronounced/dominant as the microwave processing time increases. The formation of Fe_2O_3 at shorter exposure times will be due to oxidation of Fe_3O_4. This oxidation process seems to occur during the initial rapid heating phase, from 1 to 3 minutes exposure times. Similar data (not shown here) were obtained for samples that contained 30 and 38 wt% graphite, although as expected the intensities of the graphite peaks increased with increasing waste loading. There is no significant change in crystalline phases detected in samples that were heated in air or in argon. Identical crystalline phases were also found for the sample conventionally sintered at 770ºC for 2 hours in argon.

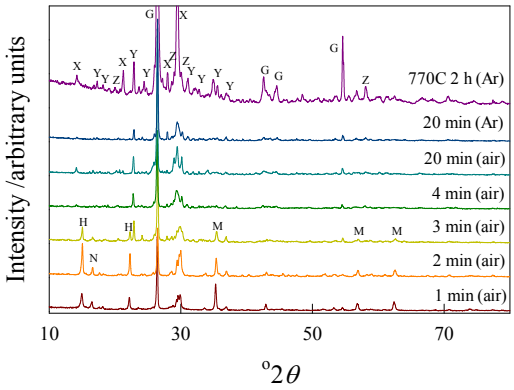

FIG 1: XRD spectra of iron phosphate glass graphite composites that contain 20 wt% graphite; G = graphite, H = Fe_2O_3, N = $NH_4H_2PO_4$, M = Fe_3O_4, X = FeP_2O_6, Y = $Fe(PO_3)_3$, Z = $Fe_2P_2O_7$

Figure 2 shows SEM micrographs of the iron phosphate glass graphite composites; Figures 2a, b and c show composites prepared using the DMO containing increasing amounts of graphite (20, 30 and 38 wt%). Rounded pores can be seen in all cases. Some evidence of lower porosity in samples prepared by conventional sintering in argon compared to the equivalent samples prepared using the DMO can be seen by comparing figures 2a and 2d. The difference in the appearance of the graphite in Figures 2a and 2d is because the graphite used in the latter case came from a different source to the former; the original source used for the DMO work having run out.

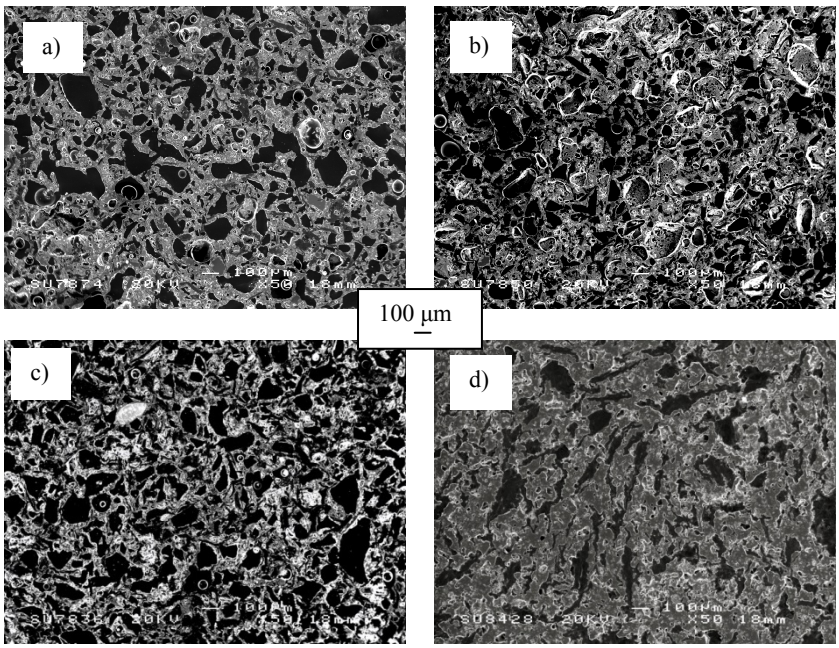

FIG 2: SEM micrographs of iron phosphate glass composites, (a) 20 minutes sample with 20 wt% graphite, (b) 20 minutes sample with 30 wt% graphite, (c) 20 minutes sample with 38 wt% graphite, (d) 20 wt% graphite sintered at 770ºC in argon

3.2 Sintering of glass-graphite composites

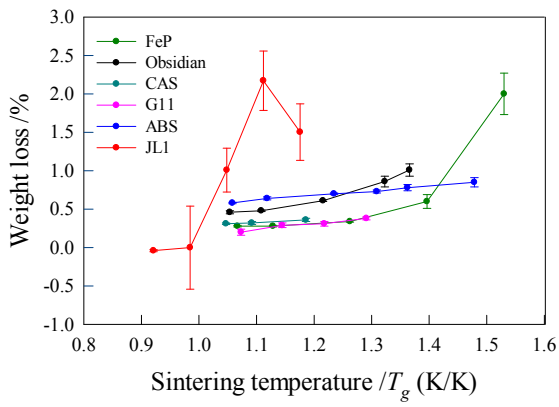

FIG 3: Weight loss as a function of sintering temperature (in K) normalised by glass transition temperature (in K) for glass 20 wt% graphite composites sintered in argon

As can be seen from Figure 3 that the weight losses for all the graphite glass composites containing 20 wt% graphite were generally under 1 wt%, except for the iron phosphate and the JL1 glass matrices at higher sintering temperatures. Some crystallisation occurs during sintering under the chosen conditions with all of the glasses (see Figure 4); with JL1, ABS-1 and obsidian being the most resistant to crystallisation.

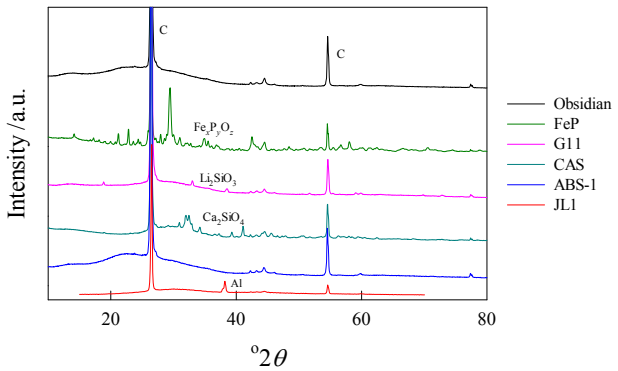

FIG 4: XRD patterns of sintered glass graphite composites showing evidence of crystallisation in all compositions as well as the presence of graphite (indicated by C). The peak marked Al is due to the aluminium sample holder.

Figure 5a shows that weight loss increases in a roughly linear fashion with increasing graphite loading. The sintering temperatures used (see Table 1) to generate the data shown in Figure 5 were those found to give maximum densification for the 20 wt% graphite samples. Although there is some indication from Figure 5a that higher weight losses are seen with higher sintering temperatures this is not completely the case as the glasses giving the lowest weight losses were sintered at 560°C (G11) and 890°C (CAS) respectively. In addition although it seems that the weight loss from the glass graphite composites increases most rapidly with the iron phosphate (FeP) glass, if the data is replotted in molar terms (Figure 5b), because the FeP glass has a much higher molar mass than all of the other glasses, the data for the FeP glass is in line with G11 and CAS glasses in the region where the mol% additions of graphite overlap.

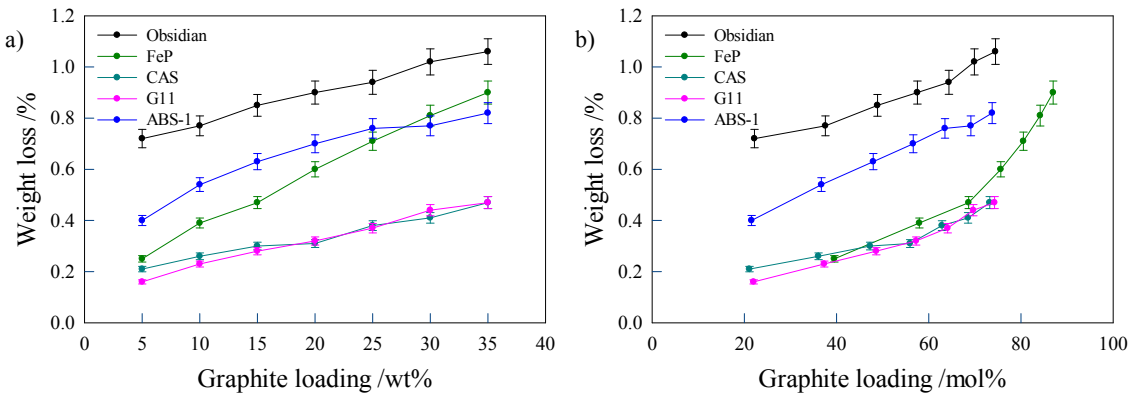

FIG 5: Weight loss as a function of graphite addition a) expressed as wt% addition and b) expressed as wt% addition (lines drawn as a guide for the eye)

It was found that the presence of graphite impeded shrinkage during sintering; when 25 wt% or greater graphite was present essentially zero densification was observed (see Figure 6). This reflects the fact that densification is only occurring place within the glassy matrix and that as the graphite volume increases this densification is impeded. The net result is that in all the glass graphite composites studied porosity remains high after pressureless sintering, so this is not an ideal route for producing graphite wasteforms.

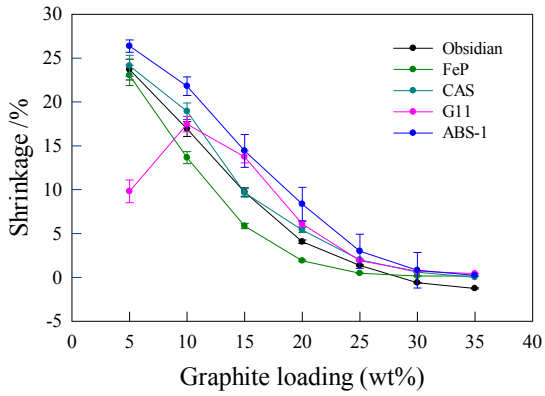

FIG 6: Shrinkage during sintering at the temperatures given in Table 1 for glass graphite composites containing varying amounts of graphite (lines drawn as a guide for the eye).

3.3 Sintering of glass-TRISO particle composites

As reported in detail elsewhere [12] cold pressing and sintering of TRISO particles and soda-lime-silica glasses in air led to complete oxidation of the outer pyrolytic carbon layer of the TRISO particles. Sintering in a mildly reducing atmosphere (95% N_2, 5% H_2) suppressed this oxidation. However, the soda-lime-silica glasses poorly wet the TRISO particles leading to a narrow gap being present between the TRISO particles and the sintered glass after sintering (see Figure 7). This is shown for an SLSA glass TRISO particle in Figure 6; similar results were obtained with SLSB and SLSC (see figure 4 in ref. [12]). In comparison as shown in Ref. [8] and Figure 8 the aluminoborosilicate (ABS) glass resulted in good wetting of the TRISO particles by the sintered glass.

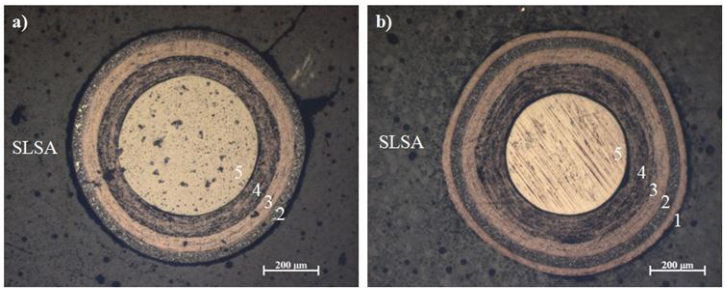

FIG 7: Optical micrographs of TRISO particle-SLSA composites sintered in a) air and b) 5% H_2/N_2 showing complete oxidation of the outer pyrolytic carbon layer in air and the lack of oxidation under a reducing atmosphere. NB: in both cases there is a gap between the TRISO particle and the glass matrix; visible all round the particle in a) and more obviously on the right hand side of the particle shown in b).

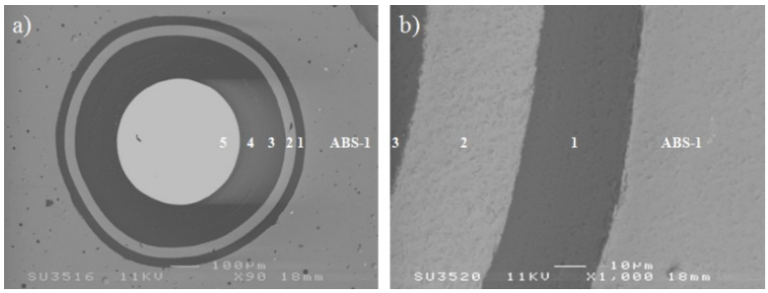

FIG 8: SEM images of ABS-1 glass TRISO particle composites sintered in 5% H_2/N_2; a) Overview showing that all 5 layers of the TRISO particle remain present and b) enlargement of the particle interface region showing good wetting of the particle by the glass

With the ABS-1 glass 10% TRISO particle composites near theoretical densities were achieved after comparatively short sintering times at low temperatures (see Table 4) with the optimum sintering conditions being 750ºC for 30 minutes.

TABLE 4: PERCENTAGE OF THEORETICAL DENSITY ACHIEVED BY SINTERING ABS-1 GLASS 10WT% TRISO PARTICLE COMPOSITES

Sintering time /min	**Sintering temperature /°C**		
	700°C	**750°C**	**800°C**
15	81 ± 1%	85 ± 1%	90 ± 1%
30	95 ± 1%	97 ± 1%	97 ± 1%
60	94 ± 1%	97 ± 1%	97 ± 1%

4. DISCUSSION

Preparation of the base 60:40 iron phosphate glass by conventional and microwave melting produced largely similar glasses, although the samples prepared in the DMO retained slightly less phosphorus than the conventionally melted sample. It was originally hoped that the short processing time required in a DMO would limit or prevent oxidation of any graphite incorporated into the glass graphite composites, however in practice greater graphite loss was found in the samples prepared using the DMO (see Table 1). This suggests that higher temperatures are reached, facilitating oxidation of graphite by reduction of the iron. Although the results for samples containing 20 wt% graphite are presented above it is worthy of note that samples that contained only 10 wt% of graphite prepared in the DMO did not retain the cylindrical shape of the green pellets; the overall pellet clearly became fluid enough for flow to occur. For graphite additions of 20 wt% or greater (essential for producing wasteforms) it seems that increasing the graphite content effectively passivates the effects of the electromagnetic wave in the DMO. The addition of 30 and 38 wt% of graphite lead to greater amounts of porosity and decreased the density of the microwaved pellets. Fundamentally, although graphite can suscept, the penetration depth of the microwaves seems to be low [13] and this limits the usefulness of microwave heating in preparing glass graphite composites.

Lower weight losses were experienced when sintering a range of glass graphite composites produced under argon atmospheres. However, with all the glasses studied it was found that using realistic amounts of graphite led to little or no densification leading to significant levels of residual porosity. While densification would be restricted by the fact that the carbon from the graphite particles is not being dissolved into the glass matrix, it is clear that the graphite does limit the densification of the glass matrix, possibly due to wetting issues (as seen with the SLS glasses and TRISO particles). In comparison densification was observed when sintering 10 wt% of TRISO particles in a reducing atmosphere either using SLS glasses or, for better wetting of the particles, an aluminoborosilicate glass (ABS-1). As shown in Ref. [8] the aluminoborosilicate base glass is also significantly more durable than the SLS glasses. Thus for higher activity carbonaceous wastes, where waste loadings will necessarily be lower, the pressureless sintering approach to produce glass-composite materials that encapsulate the waste within a durable glass remains a viable option.

5. CONCLUSIONS

Glass-graphite composites can be produced using a range of base glasses. Conventional pressureless sintering in an argon atmosphere of all the glasses was more successful in terms of graphite loss than microwave sintering with an iron phosphate base glass; the graphite did not suscept in a useful fashion which prevented the use of other glasses in the DMO. The presence of larger weight percentages of graphite impedes the production of dense glass-graphite wasteforms using the pressureless sintering

methods studied here. Successful pressureless sintering of glass TRISO particle composites was achieved, although this was only at a 10 wt% loading. This level of waste loading could be acceptable for high activity wastes (which would be the case with spent TRISO particles), however it is unlikely to be acceptable for a large volume intermediate level waste such as graphite.

6. ACKNOWLEDGEMENTS

The authors would like to thank Willie Meyer and the PBMR (South Africa) for the kind provision of TRISO particle simulant. The authors are grateful to Michael Ojovan, Claire Corkhill, Owen McGann and John Provis for their useful discussions. We thank EPRSC for part funding of this research under grant number EP/F055412/1, the Nuclear FiRST Doctoral training centre under grant reference EP/G037140/1 the E-Futures Doctoral training centre under grant reference EP/G037477/1, and University of Sheffield Knowledge Transfer Account, under grant reference EP/H500170/1. M.Z.H. Mayzan is grateful to the Ministry of Higher Education, Malaysia and Universiti Tun Hussein Onn, Malaysia for funding. N.C. Hyatt is grateful to the Royal Academy of Engineering, UK and the Nuclear Decommissioning Authority, UK for funding.

REFERENCES

[1] DONALD I.W., METCALFE B.L., and TAYLOR R.N.J., 'Review: The Immobilization of High-Level Radioactive Wastes using Ceramics and Glasses'; *J. Mater. Sci.* **32**, *pp.* 5851-5887 (1997)

[2] OJOVAN M.I., and LEE W.E., 'An Introduction to Nuclear Waste Immobilization'; Elsevier, Amsterdam (2005).

[3] JUOI J., and OJOVAN M.I., 'The Effect of Waste Loading on the Microstructure of Glass Composite Waste Forms for the Immobilisation of Spent Clinoptilolite'; *Glass Technol.: J. Europ. Glass Sci. Technol.* **48**, *pp.*124-129 (2007)

[4] MCGANN O.J., and OJOVAN M.I., 'The Synthesis of Graphite–Glass Composites intended for the Immobilisation of Waste Irradiated Graphite. *J. Nucl. Mater.* **413,** *pp.* 47-52 (2011)

[5] HEATH, P.G., CORKHILL C., HAND R.J., MADDRELL E.W., and HYATT N.C., 'Processing of Clinoptilolite Ion-Exchange Material using Hot Isostatic Pressing'; *In preparation.*

[6] HENRY N., DENIARD P., JOBIC S., BREC R., FILLET C., BART F., GRANDJEAN A., and PINET O., 'Heat Treatments *versus* Microstructure in a Molybdenum-rich Borosilicate'; *J. Non-Cryst. Solids* 333, *pp.*199-205 (2004)

[7] GODRON Y.G., 'Graphite-Glass Compositions and Method of Making the Same'; US Patent No. 3 624 005 (1971)

[8] HEATH P.G., STENNETT M.C., McGANN O.J., HAND R.J., and HYATT N.C., 'The Use of High Durability Alumino-Borosilicate Glass for Encapsulation of High-Temperature Reactor (HTR) Fuel'; Mater. Res. Soc. Symp. Proc. **1518**, mrsf12-1518-II02-02 (2013) (DOI 10.1557/opl.2013.129)

[9] MARRA J.C., 'Glass Composition Development for Stabilization of Lead-Based Paints'; US DoE report WSRC-TR-95-0479 (1996): http://www.osti.gov/bridge/servlets/purl/385594-GBrt7A/webviewable/

[10] BINGHAM P.A., HYATT N.C., and HAND R.J., 'Vitrification of UK Intermediate-Level Radioactive Wastes arising from Site Decommissioning: Property Modelling and Selection of Candidate Host Glass Compositions'; *Glass Technol.: Europ. J. Glass Sci. Technol. A* **53**, *pp.* 83-100 (2012)

[11] SCHOFIELD J.M., BINGHAM P.A., and HAND R.J., 'The Immobilisation of a Chloride-Containing Actinide Waste Surrogate in Calcium Aluminosilicate Glasses'; *Environmental Issues and Waste Management Technologies in the Materials and Nuclear Industries XII: Ceram. Trans.* **207** ed. A. Cozzi and T. Ohji *pp.* 69-80 (2009)

[12] HEATH P.G., CORKHILL C.L., STENNETT M.C., HAND R.J. MEYER W.C.H.M. and HYATT N.C., 'Encapsulation of TRISO Particle Fuel in Durable Soda-Lime-Silicate Glasses. *J. Nucl. Mater.* **436**, *pp.* 139-149 (2013) (DOI 10.1016/j.jnucmat.2013.01.285)

[13] RAJKUMAR K., and ARAVINDAN S., 'Microwave Sintering of Copper-Graphite Composites'; *J. Mater. Proc, Technol.* **209**, *pp.* 5601-5605 (2009)